X-ray diffraction analysis of cold-worked Cu-Ni-Si and Cu-Ni-Si-Cr alloys by Rietveld method

A. KHEREDDINE, F. HADJ LARBI, L. DJEBALA, H. AZZEDDINE, B. ALILI, D. BRADAI

Faculté de Physique, USTHB, BP 32 El-Alia, Dar El Beida, Alger, Algérie

Abstract: Cold worked and annealed supersaturated Cu-2.65Ni-0.6Si and Cu-2.35Ni-0.6Si-0.6Cr alloys were studied. The microstructural parameters evolution, including crystallite size, root mean square strain and dislocation density was analyzed using Materials Analysis Using Diffraction software (MAUD). The parameters for both alloys have typical values of cold deformed and subsequently annealed copper based alloy. A net change of the crystallite size, root mean square strain and dislocation density values of the alloys aged at 450 °C for 2.5−3 h seems corresponding to the recovery and recrystallization processes. Addition of Cr as quaternary element did not lead to any drastic changes of post deformation or ageing microstructural parameters and hence of recovery-recrystallization kinetics.

Key words: Cu-Ni-Si alloy; microstructure; XRD line profile analysis; Materials Analysis Using Diffraction software

1 Introduction

Copper-base alloys present both high strength and high electrical conductivity required in electronic fields such as the framework of IC and connectors. Nowadays, Cu-Ni-Si alloys with small addition of other elements[1−8] have recently created a great interest. The thermo mechanical processing of these alloys is based on the plastic deformation by cold rolling and a subsequent ageing treatment. Even if a consequent documentation about the microstructural evolution as well as electrical and mechanical properties has been assembled yet, a manifest lack exists concerning the post deformation microstructural features like crystallite size, root mean square strain and dislocation density. It is well known that these parameters are the key factors controlling the microstructure evolution during annealing.

In this work, an extensive evaluation of the microstructural parameters after evolution upon cold rolling and ageing of supersaturated Cu-2.65Ni-0.6Si and Cu-2.35Ni-0.6Si-0.6Cr (mass fraction, %) solid solutions was studied. Three cold plastic deformation levels, 70%, 90% and 95% (thickness reduction) were investigated and X-ray diffraction line profile analysis was carried out using JAVA-based Materials Analysis Using Diffraction (MAUD) 2 software[9−10].

2 Experimental

The Cu-2.65Ni-0.6Si and Cu-2.35Ni-0.6Si-0.6Cr (mass fraction, %) alloys were provided by Le Bronze Industriel Firma (France) in the form of cylinders. Ingots (Parallelepipeds) were cut from the alloys and sealed in quartz capsules, then homogenized at 850 °C for 2 h and water quenched. The alloys were cold rolled to thickness reductions of 70%, 90% and 95%, and then aged at 450 °C in a time range from 0.5 to 9 h. Flat diffractometer specimens were prepared from Cu-2.65Ni-0.6Si and Cu-2.35Ni-0.6Si-0.6Cr alloys. The X-ray diffraction patterns were recorded from the rolled and polished surface using BRUKERS D8 ADVANCE X-ray diffractometer operating at 40 kV, 40 mA with Cu K_α radiation. All the diffraction patterns were obtained by varying 2θ from 15° to 88° with a scan step of 0.05. The time spent for collecting the data per step was 1.5 s.

3 Methodology

In this work, MAUD software which is based on a Rietveld refinement procedure was used[9−10]. This refinement procedure is fundamentally based on the use of analytical functions of pseudo-Voigt[11] and Pearson VII to model the whole experimental XRD patterns. A

diffraction pattern was simulated with all the fitting parameters (structural, microstructural, peak shape, width and background) and compared to the experimental data. The Rietveld's refinement adopted an iterative least square procedure through minimization of the residual parameter. Capabilities and limitations of the Rietveld's refinement from XRD data were widely discussed[12]. The Popa's model of anisotropic size-strain broadening was used for the evaluation of the crystallite size and the microstrain values[13]. The direction dependent crystallite size (R_h) is developed in a convergent series of symmetrized spherical harmonics $K_{2l}^\mu(\Phi, \varphi)$, as shown in Eq.(1).

$$R_h = R_0 + R_1 K_4^1(\Phi, \phi) + R_2 K_6^1(\Phi, \phi) + R_3 K_6^1(\Phi, \phi) + \cdots \tag{1}$$

where the coefficients R_i are refinable parameters; the symmetrized spherical harmonics are the combination of functions $P_{2l}^m(x)\cos m\varphi$ ($P_{2l}^m(x)$ is the normalized Legendre function of argument x=cos Φ); Φ and φ are the polar and azimuthal angles in an orthogonal coordinate system, respectively.

The (h,k,l)-dependent strain Popa's model for cubic symmetry is given as:

$$\varepsilon_{hh}^2 E_H^4 = E_1(h^4 + k^4 + l^4) + 2E_2(h^2 k^2 + k^2 l^2 + l^2 h^2) \tag{2}$$

where coefficients E_1 and E_2 are the combination of terms like ($\varepsilon_{ij}\varepsilon_{mn}$). The relative change of interplanar distance produced by stress is given by $\varepsilon_{hh} = -\Delta H / H$, in which H is one direction of the reciprocal lattice vector of unit vector h. ε_{hh} represents the (h, k, l)-dependent macroscopic strain, producing a peak shift.

In the calculation, the crystallite size is given by the diameter rather than the radius as expressed in Eq.(1) and the microstrain is the square root of ε_{hh}^2 parameter of the Popa's model.

4 Results and discussion

Figure 1 presents the XRD pattern obtained from supersaturated Cu-2.65Ni-0.6Si alloy with the presence of three first characteristic diffraction peaks (111), (200) and (220) of an FCC structured Cu matrix. There is no appearance of other peaks belonging to probable precipitate phases like Ni_2Si or $(Cu, Ni)_3Si$. Figures 2 and 3 show the X-ray diffraction patterns of the cold rolled samples and the ones aged at 450 °C for different periods of time of the Cu-2.65Ni-0.6Si and Cu-2.35Ni-0.6Si-0.6Cr alloys, respectively. The X-ray diffraction patterns of all the specimens were subjected to detailed microstructural studies using MAUD software, as evoluted by plastic deformation and aging. These samples show higher lattice parameter values (listed in Table 1), revealing shifted reproduced peaks are mainly
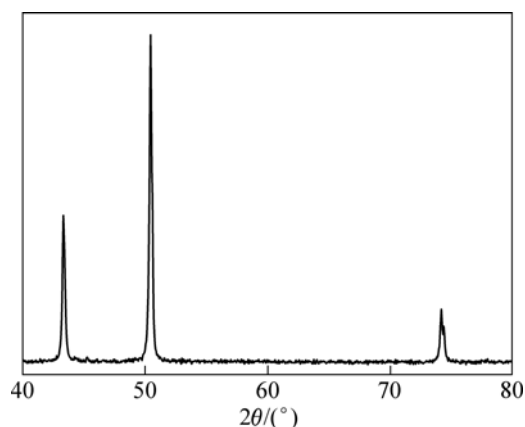

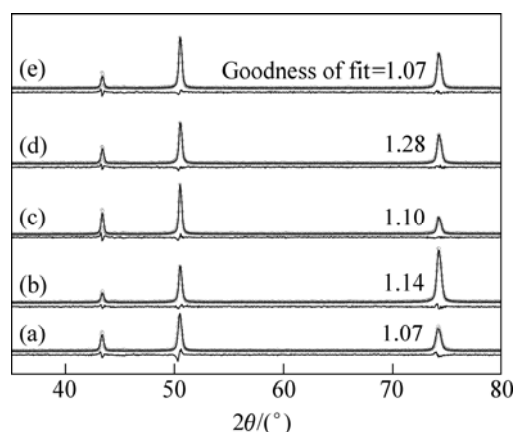**Fig.1** XRD pattern of supersaturated Cu-2.65Ni-0.6Si alloy

Fig.2 XRD patterns obtained from Rietveld profile fitting of Cu-2.65Ni-0.6Si alloy deformed with thickness reduction of 70%: (a) As cold-worked sample; (b) Aged at 450 °C for 1 h; (c) Aged at 450 °C for 3 h; (d) Aged at 450 °C for 6 h; (e) Aged at 450 °C for 9 h (Lower lines represent residue of experimental and fitted patterns)
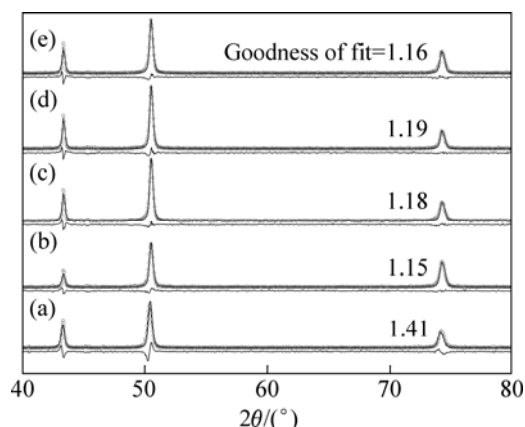

Fig.3 XRD patterns obtained from Rietveld profile fitting of Cu-2.35Ni-0.6Si-0.6Cr alloy deformed with thickness reduction of 70%: (a) As cold-worked sample; (b) Aged at 450 °C for 1 h; (c) Aged at 450 °C for 3 h; (d) Aged at 450 °C for 6 h; (e) Aged at 450 °C for 9 h (Lower lines represent the residue of experimental and fitted patterns)

Table 1 Lattice parameter of Cu-2.65Ni-0.6Si and Cu-2.35Ni-0.6Si-0.6Cr alloys aged at 450 °C (Å±0.006)

Alloy	Thickness reduction/%	Aging time				
		As cold rolled	1 h	3 h	6 h	9 h
Cu-2.65Ni-0.6Si alloy	70%	3.617	3.612	3.611	3.611	3.612
	90%	3.616	3.611	3.612	3.612	3.612
	95%	3.615	3.612	3.612	3.612	3.613
Cu-2.35Ni-0.6Si-0.6Cr alloy	70%	3.613	3.612	3.613	3.611	3.612
	90%	3.616	3.613	3.616	3.614	3.613
	95%	3.618	3.613	3.612	3.612	3.613

caused by the solute effects rather the deformation which does not change the parameters.

In case of deformed samples, Rietveld analysis required a correction due to the effect of texture[14−15]. The parameter of gross preferential orientation has a value close to 0.6, which indicates the existence of a strong preferred orientation within the material.

The lattice parameters of the deformed solid solution seem also stable and are located at 3.612 and 3.613 Å, respectively. The higher value for the Cu-2.35Ni-0.6Si- 0.6Cr solid solution seems due to the effect of Ni content and the addition of Cr. A similar effect of Cr was evoked in Ref.[16]. Indeed, it was evidenced that Cr (anti ferromagnetic element) increases the expansion coefficient and the lattice parameter.

Figure 4 presents the evolution of the crystallite (coherent domains of diffraction) size versus deformation (cold rolling) level and annealing temperature for supersaturated Cu-2.65Ni-0.6Si and Cu-2.35Ni-0.6Si-0.6Cr solid solutions.

For both alloys, a global decrease of the size of coherent domains with the deformation level and an increase with ageing time are observed. It is known that the more a metallic material deforms, the more the size of the coherent domains decreases, while an annealing tends to increase it by recovery-recrystallization mechanism on the contrary. For both alloys, the crystallite size values are comparable and a net change for around 2.5−3 h aging is depicted. This temperature range may correspond to a recovery-recrystallization time.

Figure 5 presents the evolution of the root mean square strain versus deformation (cold rolling) level and annealing temperature for supersaturated Cu-2.65Ni-0.6Si and Cu-2.35Ni-0.6Si-0.6Cr solid solutions. The micro distortions in both alloys slightly increase with deformation level and decrease with ageing time. The drop of the micro distortions is less pronounced when the deformation level increases. Globally the micro distortions values are not different for both the studied

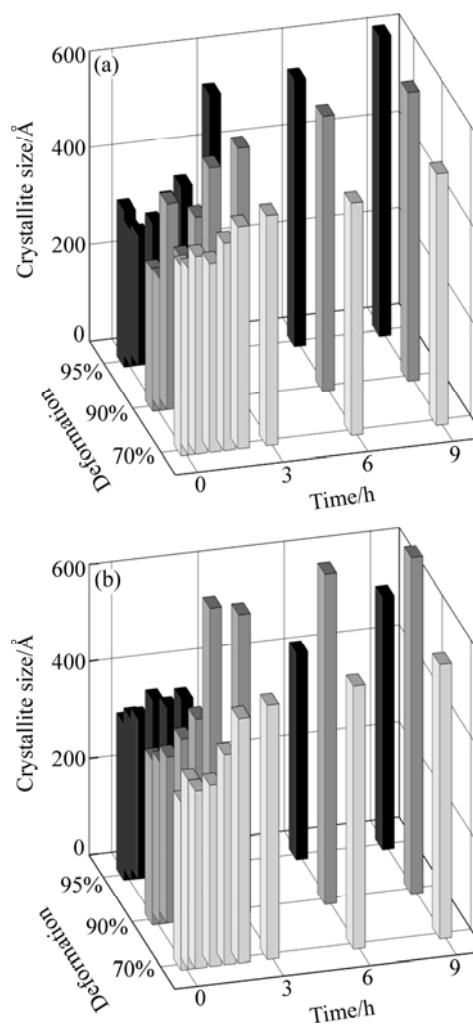alloys and the same net change aged for around 2.5−3 h is depicted in Fig.4.

Fig.4 Evolution of crystallite size versus deformation (cold rolling) level and annealing temperature for supersaturated Cu-2.65Ni-0.6Si (a) and Cu-2.35Ni-0.6Si-0.6Cr (b) solid solutions

Figure 6 presents the evolution of the dislocations density versus deformation (cold rolling) level and ageing time for supersaturated Cu-2.65Ni-0.6Si and Cu-2.35Ni-0.6Si-0.6Cr solid solutions. It is noticed that there is an overall increase of the dislocation density with the deformation level and a global decrease with the ageing time. The increase is explained by a work hardening mechanism upon cold rolling by continued trapping of newly created mobile dislocations, existing dislocations and their incorporation into the various microstructural features[17]. The decrease of the density during the ageing is explained simply by a mechanism of progressive dislocation annihilation via recovery and recrystallization.

From Fig.6, it is noticed that the dislocation density of Cu-2.35Ni-0.6Si-0.6Cr alloy is smaller than that of
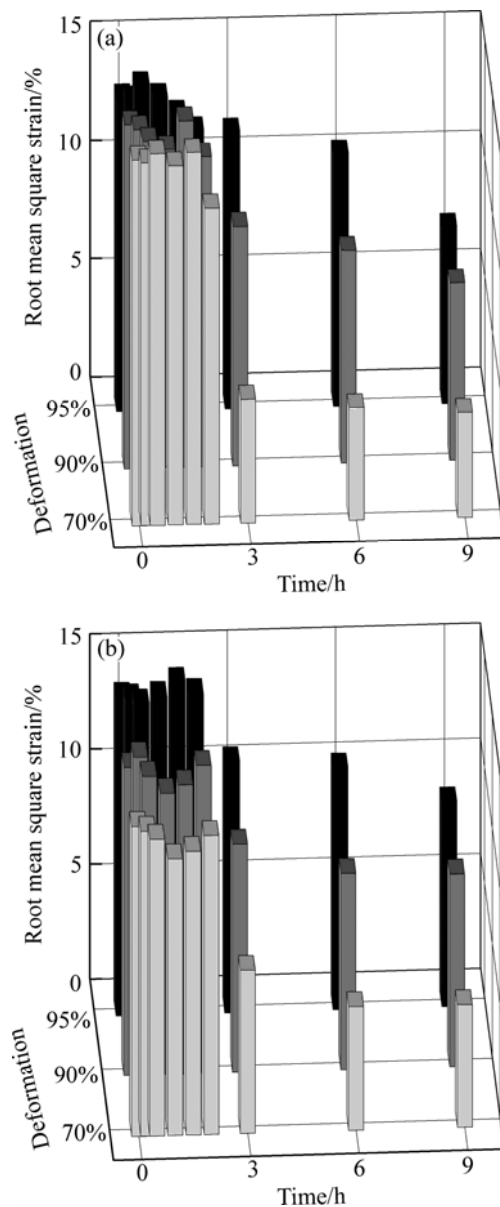
Fig.5 Evolution of root mean square strain versus deformation (cold rolling) level and annealing temperature for supersaturated Cu-2.65Ni-0.6Si (a) and Cu-2.35Ni-0.6Si-0.6Cr (b) solid solutions

Cu-2.65Ni-0.6Si alloy. This may be attributed to the presence of Cr additions that exert a pinning effect on the dislocation motion. A similar effect was observed in Al-Mg alloy[17].

The sizes of crystallites (coherent domains of diffraction) are in the same order between 289−619 Å for Cu-2.65Ni-0.6Si alloy and 325−696 Å for Cu-2.35Ni-0.6Si-0.6Cr alloy, respectively. Micro distortions seem to evolve in the same way and in a range of (4.4−15.4)×10⁻⁴ for Cu-2.65Ni-0.6Si and (5.3−13.8)×10⁻⁴ for Cu-2.35Ni-0.6Si-0.6Cr alloys, respectively.

The dislocation densities evolve in the same way for both alloys and their values are $(0.24−1.72)×10^{11}$ cm^{-2} for Cu-2.65Ni-0.6Si and $(0.28−1.31)×10^{11}$ cm^{-2} for Cu-2.35Ni-0.6Si-0.6Cr alloy, respectively.

It can be assumed that the chromium addition to ternary Cu-Ni-Si alloy does not yield significant changes of the post deformation and annealing microstructural parameters. As pointed out in Ref.[17], this element is rather added for metallurgical purposes to improve the plastic properties.

SAHU et al[18] reported the results of a similar study on Cu-15Ni-(5, 8, 13) Sn (mass fraction, %). It is noted that no indication on the deformation level of their alloys was given. The results are more or less similar to this research. However, it was determined that higher dislocation densities $(10^{-12}$ cm$^{-2})$ increased gradually with the increase of Sn content in the alloy. Maybe the
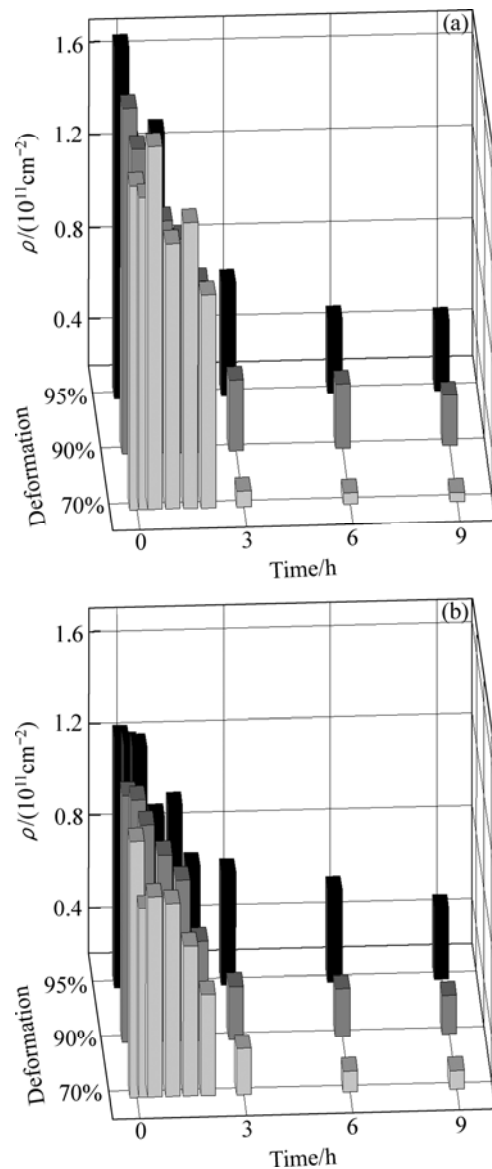

Fig.6 Evolution of dislocation density versus deformation (cold rolling) level and annealing temperature for supersaturated Cu-2.65Ni-0.6Si (a) and Cu-2.35Ni-0.6Si-0.6Cr (b) solid solutions

plastic deformation method (hand filling) could introduce much higher dislocations into the material. Indeed, the substitution of Sn by Si and addition of Cr seem to lead to any drastic changes of post deformation and annealing microstructural parameters and hence of recovery-recrystallization kinetics.

The lattice parameter of supersaturated Cu-Ni-Sn alloys determined by SAHU et al[18] was around 3.621 Å. This value is higher than that of the present study, which may arise from a combined effect of substitution of Sn by Si and addition of Cr. The lattice parameter of Cu-xNi (x varying from 0 to 100%) was determined by ALILI et al[19]. The Cu-Ni solid solution was found to obey Végard's law and the lattice parameter decreased from 3.609 to 3.601 Å when the Ni content increased from 5% to 15%. Hence, the addition of Sn, Si and Cr elements increased the lattice parameter of Cu-Ni solid solution.

The crystallite size values of deformed alloys determined by SAHU et al[18] were lower than those of the present study (100 Å and 289−325 Å, respectively). For the annealed alloys, the values are more or less comparable (450-750 Å and 619-696 Å, respectively). Micro distortion values determined by SAHU et al[18] are lower than those of the present study (15.4×10^{-4} and 60×10^{-4}, respectively).

The dislocation densities of the deformed Cu-2.65Ni-0.6Si and Cu-2.35Ni-0.6Si-0.6Cr alloys were in range of $(0.21-1.72) \times 10^{11}$ cm^{-2} while those of Cu-Ni-Sn studied by SAHU et al[18] and Cu-Ni-Zn[20] were around 8×10^{11} and 18×10^{11} cm^{-2}, respectively. If it is assumed that the amount of deformation is the same, these differences may be due to the segregation difference of elements Sn, Si and Cr in grain boundaries in one hand and clustering in other hand, which determines the dislocation mobility.

The net change depicted in Figs.4 and 6 is in agreement with the results in Ref.[2], in which around 80% of the maximum conductivity was restored between 1 and 4 h of ageing depending on the initial treatment of the alloy. It is evidenced a slow rise in the electrical conductivity of the alloy aged for up to 12 h and then a nearly constant value with further increase in ageing time up to 35 h.

Several works[3] showed that the hardness of the aged Cu-Ni-Si alloys was increased by cold rolling after solution treatment. This phenomenon is considered to result from preferential precipitation in high density of dislocations introduced by cold rolling. The finely dispersed precipitates which are responsible for the high performance are identified as δ-Ni$_2$Si[21]. Ageing at 450 °C induces combined precipitation and recovery-recrystallization reactions that are similar to the third part of the scheme proposed by HORNBOGEN and KÖSTER[22], in which precipitation occurs before recrystallization. The δ-Ni$_2$Si particles precipitate continuously and control the recovery rate. Subsequent discontinuous precipitation of Ni$_2$Si occurs on migrating high angle grain boundaries.

5 Conclusions

1) Cu-2.65Ni-0.6Si and Cu-2.35Ni-0.6Si-0.6Cr alloys were cold deformed and subsequently aged at 450 °C for a time period ranging from 0.5 to 9 h. The crystallite size, root mean square strain and dislocation density are typical parameters.

2) A net change of the crystallite size, root mean square strain and dislocation density values of aging at 450 °C for 2.5−3 h seems to correspond to the recovery and recrystallization processes.

3) Addition of Cr as quaternary element does not lead to any drastic changes of post deformation and aging microstructural parameters and hence of recovery-recrystallization kinetics.

References

[1] ZHAO D M, DONG Q M, LIU P, KANG B X, HUANG J L, JIN Z H. Structure and strength of the age hardened Cu-Ni-Si alloy [J]. Materials Chemistry and Physics, 2003, 79(1): 81−86.

[2] SRIVASTAVA V C, SCHNEIDER A, UHLENWINKEL V, OJHA S N, BAUCKHAGE K. Age-hardening characteristics of Cu-2.4Ni-0.6Si alloy produced by the spray forming process [J]. J Mater Process Tech, 2004, 147(2): 174−180.

[3] SUZUKI S, SHIBUTANI N, MIMURA K, ISSHIKI M, WASEDA Y. Improvement in strength and electrical conductivity of Cu-Ni-Si alloys by aging and cold rolling [J]. Journal of Alloys and Compounds, 2006, 417(1−2): 116−120.

[4] LEBRETON V, BARBEAU F, BIENVENU Y. Precipitation in CuNi15wt%Sn8wt% and CuNi6wt%Si1.8wt% Alloys [C]// Proceedings of the International Conference Copper'06. France: UTC Compiègne, 2006: 86−92.

[5] MONZEN R, WATANABE C. Microstructure and mechanical properties of Cu-Ni-Si alloys [J]. Materials Science and Engineering A, 2008, 483−484(1−2): 117−119.

[6] PAN Zhi-yong, WANG Ming-pu, LI Zhou, XIAO Zhu, CHEN Chang. Thermomechanical treatment of super high strength Cu-8.0Ni-1.8Si alloy [J]. Transactions of Nonferrous Metals Society of China, 2007, 17(11): 1821−1826.

[7] WATANABE C, NISHIJIMA F, MONZEN R, TAZAKI K. Mechanical properties of Cu-4.0wt%Ni-0.95wt%Si alloys with and

without P and Cr addition[J]. Material Science Forum, 2007, 561−565(114): 2321−2324.

[8] SUN Z, LAITEM C, VINCENT A. Dynamic embrittlement at intermediate temperature in a Cu-Ni-Si alloy [J]. Materials Science and Engineering A, 2008, 477 (1): 145−152.

[9] LUTTEROTTI L. MAUD. CPD NEWSLETTER, (IUCr), December 2000, 24.

[10] MAUD: Material Analysis Using Diffraction, http://www.ing.unitn.it/~luttero/.

[11] HADJ L F, KHEREDDINE A, ALILI B, BRADAI D. Généralisation des expressions analytiques liées a la fonction pseudo-voigt utilisée en analyse des profils de raies de diffraction [J]. FIZIKA , 2009, 18A (2): 63−72. (in French)

[12] YOUNG R A. The Rietveld method [M]. UK: Oxford University Press, 1993: 1−38.

[13] POPA N C. The (hkl) dependence of diffraction-line broadening caused by strain and size for all laue groups in rietveld refinement [J]. J Appl Cryst, 1998, 31(2): 176−180.

[14] MARCH A. Mathematische theorie der rege- lung nach der korngestalt bei affiner deformation [J]. Z. Kristallogr, 1932, 81: 285−297.

[15] DOLLASE W A. Correction of intensities for preferred orientation in powder diffractometry: application of the March model [J]. J Appl Crystallogr, 1986, 19(4): 267−272.

[16] JULLIARD F. Study of recrystallization mechanisms in the Invar, Fe-36%Ni alloy. UK, T 139597 [P]. 2001.

[17] HUMPHREYS F J, HATHERLY M. Recrystallization and related annealing phenomena [M]. Oxford, UK: Pergamon, 1995: 12−14.

[18] SAHU P, PRADHAN S K, DE M. X-ray diffraction studies of the decomposition and microstructural characterization of cold-worked powders of Cu-15Ni-Sn alloys by Rietveld analysis [J]. Journal of Alloys and Compounds, 2004, 377(1−2): 103−116.

[19] ALILI B, RAHO A, KADI-HANIFI M. Étude de la variation du paramètre de réseau de solutions solides Cu-Ni par diffraction des rayons X [J]. J Phy IV France, 2004, 118: 409−411. (in French)

[20] HALDER S K, DE M, SEN GUPTA S P. An X-ray diffraction study on the microstructures of cold-worked fcc Cu-Ni-Zn alloys [J]. J Appl Phy, 1977, 48(8): 3560−3565.

[21] LONG Yong-qiang, LIU Ping, LIU Yong, ZHANG Wei-min, PAN Jian-sheng. Simulation of recrystallization grain growth during re-aging process in the Cu-Ni-Si alloy based on phase field model [J]. Materials Letters, 2008, 62(17−18): 3039−3042.

[22] HORNGOGEN E, KÖSTER V. Recrystallization of Metallic Materials [M]. Stuttgart: Dr. RiederVerlag, 1978: 159.

冷加工 Cu-Ni-Si 和 Cu-Ni-Si-Cr 合金的分析

A. KHEREDDINE, F. HADJ LARBI, L. DJEBALA, H. AZZEDDINE, B. ALILI, D. BRADAI

Faculté de Physique, USTHB, BP 32 El-Alia, Dar El Beida, Alger, Algérie

摘　要：研究经冷加工和退火处理的过饱和 Cu-2.65Ni-0.6Si 和 Cu-2.35Ni-0.6Si-0.6Cr 合金。采用软件 MAUD 分析其显微组织参数的演变，包括晶粒尺寸、应变均方根和位错密度等。结果表明，经过冷加工和退火处理的两种合金的显微组织参数都具有特定值。在 450 ℃时效 2.5~3 h 的合金，其晶粒尺寸、应变均方根和位错密度等参数的净变化量与回复和再结晶过程相关。Cr 作为第四组元添加到合金中没有明显改变形变和时效处理后合金的结构参数，因此也不影响合金的回复再结晶动力学。

关键词：Cu-Ni-Si 合金；显微组织；XRDLPA；Materials Analysis Using Diffraction 软件

(Edited by FANG Jing-hua)